LA-UR -84-2003

Los Alamos National Laboratory is operated by the University of California for the United States Department of Energy under contract W-7405-ENG-36

LA-UR--84-2003

DE85 008627

TITLE: PERFORMANCE OF AN ACTIVE/PASSIVE HYBRID SOLAR SYSTEM UTILIZING VAPOR TRANSPORT

OK
DT

AUTHOR(S): James C. Hedstrom

MASTER

SUBMITTED TO Informal Distribution

DISCLAIMER

Los Alamos Los Alamos National Laboratory
Los Alamos, New Mexico 87545

FORM NO 836 R4
ST NO 2629 5/81

PERFORMANCE OF AN ACTIVE/PASSIVE HYBRID SOLAR SYSTEM UTILIZING VAPOR TRANSPORT*

by

James C. Hedstrom
Los Alamos National Laboratory
Los Alamos, New Mexico 87545

ABSTRACT

Vapor-phase heat-transport systems are being tested in two of the passive test cells at Los Alamos. The systems consist of an active fin-and-tube collector and a condenser inside a water storage tank. The refrigerant, R-11, can be returned to the collector with a pump or with a self-pumping scheme. A computer model was developed to predict the behavior of the system, after which we used the computer to predict the annual performance of these systems in five cities. The report compares the measured and the predicted results as well as the system's sensitivity to several parameters.

INTRODUCTION

Vapor-transport systems can offer performance improvements over current active and passive solar energy space heating systems because of higher heat-tranfer rates obtained in the evaporation and condensation process and lower heat losses at night. We are currently investigating a system consisting of an active-type solar collector with passive water storage. The passive discharge operates at lower temperatures, thereby improving performance. Previous system studies have shown substantial improvements in

---

*Work performed under the auspices of the US Department of Energy, Office of Solar Heat Technologies.

performance over other passive systems.[1,2] Moreover, vapor systems should have simpler controls than conventional active systems and, therefore, improved reliability.

In this program, we are addressing situations in which locating the collector below the condenser is not feasible, such as systems with collectors on the south side of a building or on the roof with storage units within the occupied space.

The first system we built has the collector on the south wall of Test Cell 8 with all piping and accumulators inside the test cell. We have run the collector both vertically and tilted at latitude. Early results from this system were reported in Ref. 3. More complete performance data and computer validation on this system are the subject of this report.

A second self-pumping system with the collector on the roof of Test Cell 7 has been in operation since December 1983. The performance of this system is being evaluated.

DESCRIPTION OF EXPERIMENT

A schematic of the vapor-transport system built into Test Cell 8 is shown in Fig. 1. One selective-surface, single-glazed collector with a gross area of 24.2 ft^2 (aperture area 22.4 ft^2), with a copper absorber plate and 3/8-in. copper tubes spaced 2 in. on center, was mounted on the south wall. The water tank inside the test cell measures 36 in. by 12 in. by 96 in. high. It was filled to a depth of 78 in. for a total volume of 154 gallons. The condenser submersed in the water was a coil of 3/8-in. i.d. copper tubing approximately 16 ft long; the piping connecting the various components on the system was 1/2-in. o.d. hard copper tubing. The pump, grossly oversized for this particular experiment, was a positive-displacement diaphragm type with a constant flow rate of 2 gpm. We controlled the pump with a float switch in a receiver on the inlet of the pump.

We have also operated a self-pumping mode, as shown in the schematic in Fig. 2. The condensate in the condenser flows through the check valve and up into the accumulator because of the lower saturation temperature and pressure in the accumulator. To dump the liquid in the accumulator back into the collector we must equalize the pressure on both sides of the loop by opening a solenoid valve that is operated by an electric float switch inside the accumulator. The hot gas from the collector must condense and cool in the

accumulator before the cycle can be repeated. The heat lost from the accumulator is delivered directly to the room. The check valves used in the self-pumping configuration were in-line, 3/8-in. refrigerant, spring-loaded check valves.

All of the test cells have electric heaters controlled by the computer-based, data-acquisition system; the room temperature of each cell is scanned every 20 seconds. When the temperature drops below the setpoint, the heater is turned on. The cells have a controlled infiltration of four air changes per hour.

EXPERIMENTAL RESULTS

Several temperatures in the test cell are illustrated in Fig. 3 with the system in the self-pumping mode. The plots show the following: the temperature of the absorber surface measured 7 in. from the top of the collector, the saturation temperature calculated from the pressure measured at the collector outlet, the temperature measured at the top of storage, the room temperature, and the ambient temperature. The collector surface temperature is a maximum of 7°F higher than the saturation temperature and is 42°F higher than the storage temperature at noon. The saturation temperature and the temperature at collector outlet are essentially identical. The average daily swing in storage temperature is 1°F.

The test cell was maintained at a minimum setpoint of 65°F with auxiliary heat. A detailed plot of the various temperatures measured in the test cell is shown in Fig. 4. The plot shows the cycling of the system increase to a maximum at noon. The collector is seen to dry out at the beginning and the end of the day as the cycling stops. The pressures measured on the collector and accumulator sides of the loop are plotted in Fig. 5. The pressure difference shown in Fig. 6 is about 5 psi except when the system dumps; 5 psi is the required pressure head to lift the liquid 8 feet up into the accumulator.

The alternate mode of operation involves returning the liquid to the collector with a pump. This mode guarantees that the collector is full and the condenser is dry. The pump is controlled by a float switch in the receiver at the pump inlet. Typically, the pump will run a maximum of 3 seconds every 2-1/2 minutes, resulting in a minimal amount of electrical energy usage. A 2-day temperature plot with the system in this mode is shown

in Fig. 7. The temperature behavior is almost identical to that of the self-pumping mode. The temperature measured 12 in. from the bottom of the storage tank is about 10°F hotter in this mode than in the self-pumping mode, indicating that the condenser is dryer.

Daily performance is determined by an energy balance on the test cell. The solar energy delivered to each test cell is determined by subtracting the auxiliary energy and any change in stored energy from the test cell heat loss; the load coefficients for each test cell are determined by nonsolar load calibration tests. More details may be found in Refs. 4 and 5. Load calibration tests were performed February 3-8, 1984, by covering the collectors and valving off the system. The daily collector output or amount of energy delivered to the test cell is shown in Fig. 8 as a function of daily solar radiation incident on the collector. The average efficiency (output/incident) for the month of January 1984 was 45%; efficiency when the incident solar radiation is 2000 Btu/ft^2 day is 49%. The performance from January 1-11 and from January 15-31 was identical, proving that the self-pumping mode and the mechanical-pumping mode performed nearly the same.

DESCRIPTION OF COMPUTER MODEL

A computer code used previously for active liquid system studies (Refs. 6-9) was modified to simulate an active/passive hybrid system with vapor transport. The code is a system of equations solved hourly to obtain an energy balance on the system. The hourly energy terms are summed into daily, monthly, and yearly energy quantities.

A schematic of the model's parameters is shown in Fig. 9. The code calculates the collector output, knowing the condenser temperature, the ambient temperature, and the incident solar radiation. The pipe losses to both the outdoors and indoors are then subtracted from the collector output to obtain the storage input. An energy balance is performed on the storage to obtain a new hourly storage temperature. An energy balance is likewise performed on the room to obtain a new hourly room temperature.

The collector model consists of an energy balance on the collector. First we calculate the energy incident on the absorber surface by accounting for the reflectance and the absorptance of the glazing. An estimated absorber temperature is then used to calculate the convective heat loss, the radiation heat loss, the back-side heat loss, and the energy stored in the collector

since the previous hour. The collector output is calculated from the difference between the absorber temperature and the storage temperature and a coefficient derived from the collector flow rate, the heat-transfer coefficient between the absorber and the fluid, and the heat-transfer coefficient of the condenser. We then iterate on the absorber temperature to obtain an energy balance.

Room temperature is controlled to an upper-bound temperature (TRMMAX) by venting energy from the space when the upper bound is reached. Likewise, a lower-bound temperature is controlled by adding auxiliary heat to the room.

VALIDATION RESULTS

The data set chosen for the validation study was the month of January 1984. The vapor system in Test Cell 8 was run in the self-pumping mode for the first 11 days of the month and in the mechanical-pumping mode the remainder of the month. Various problems in the data were encountered on January 12, 14, and 27, so that they were left out of the comparison.

The comparison of the daily results is given in Table I and Figs. 10, 11, and 12. This is a comparison of the daily measured results that were obtained by an energy balance on the test cell as explained above. The overall agreement, as shown by the totals in Table I, is excellent. The collector output agrees within 1%, the load agrees within 3%, and the auxiliary agrees within 5%. The building load coefficient was identical to the value (28.3 Btu/h °F) used to determine the experimental heat loss from the test cell. The difference in the totals is attributable to the difference in the measured and calculated room (cell) temperatures. The measured hourly solar radiation was used to drive the simulation model. The meaningful calculated parameter is the collector output, which can be adjusted by selecting the appropriate input parameters.

Comparison of calculated and measured hourly results was also made. The parameters compared were the absorber temperature (TC), the collector outlet temperature (TCOUT), the average storage temperature (TS), and the room temperature (TRM). The first 16 days are shown in Figs. 13a-d and the last 16 days of the month are shown in Figs. 14a-d. On this broad scale we see that the agreement is very good. Furthermore, there seems to be no difference between the first part of the month in the self-pumping mode and the last part of the month when the pump was operating. A more detailed comparison is shown

for January 7-8 in Figs. 15a-d and for January 24-25 in Figs. 16a-d. These plots show a lag of about 1 hour in the calculated values behind the measured values.

The final parameters selected in this validation process are given in Table II. Various input parameters were adjusted to obtain a reasonable comparison between the calculated and measured results while keeping the input parameter within some realistic values. The collector absorber and outlet temperatures could be adjusted by varying the condenser heat-transfer coefficient (UH). The collector heat output also varied with this parameter. A final value of UH = 7 Btu/h ft_c^2 °F seemed to give the best result. This parameter is a function of the actual dry condenser area and the heat-transfer coefficient between the condenser tube o.d. and the water. The condensation heat-transfer coefficient on the tube i.d. should be much higher and, therefore, not contribute to the overall thermal resistance.

The collector heat output (qcout) could also be adjusted by varying the absorptivity (ALF) of the collector absorber surface. A lower value of 0.90 was used (manufacturer's published value was 0.95) to decrease the collector output to the apparent measured output.

The storage temperature swing was adjusted with the storage heat capacity term (SCPM). The total heat capacity of storage was about 55 Btu/h °F in the test cell, but only 45 Btu/h °F was determined to be effective. The temperature level of storage was adjusted by varying the heat transfer between the storage and the room (US). The value that gave the best agreement with measurements was about 1.5 Btu/h °F ft_c^2, which seemed a little low. The storage tank, however, was bright aluminum with two sides against the corner of the test cell, conditions that make practical evaluation of this parameter difficult.

Because the pipes and the various accumulators inside the test cell are uninsulated, a sizable fraction of the heat from the system is dumped directly into the room. The parameter controlling the heat flow in the simulation model is the second pipe heat-loss coefficient (UP2). A rather large value of 0.6 Btu/h °F ft_c^2 was used to obtain a fair comparison of measured and calculated room temperatures.

The computer simulation model described above and the input parameters that went into it seem to give a good prediction of the performance of an actual vapor-transport system. Further work on the model will probably

provide a better understanding of systems of this type; however, the computer program and the model, at this point, seem adequate to provide a realistic annual performance estimate of this system for several climates.

SENSITIVITY STUDIES

Following the validation study, a sensitivity study was conducted to determine the performance of a vapor transport system in several climates. The cities chosen for analysis were the four cities used in the Active Program Research Requirement (APRR) Residental Systems Evaluation. These cities were Madison, Wisconsin; Washington, D.C.; Phoenix, Arizona, and Denver, Colorado. In addition, Albuquerque was included because of its proximity to Los Alamos and its ideal climate for solar heating.

The base case parameters for this study are included in the second column of Table II. In general the same parameters were used as in the validation study except for the parameters involving the storage geometry and the pipe heat loss to the room. For this study we assumed that the storage would consist of 18-in.-diameter tubes filled with water. With a heat storage capacity of 45 Btu/h ft_c^2 and a heat-transfer coefficient between the storage surface and the room of 1.5 Btu/h °F ft_c^2, the value of US would be 4.0 Btu/h °F ft_c^2. In addition, the number of uninsulated pipes inside the room was assumed to be small so that a value of UP2 = 0.1 was assumed instead of the value of 0.6 used in the validation study.

The sensitivity study involved the variation of five input parameters: the collector area (AC), collector tilt (TILT), storage heat capacity (SCPM), storage heat-transfer coefficient (US), and condenser heat-transfer coefficient (UH).

The results for the parameter variation of collector area are given in Table III and in Figs. 17a-c. A house with a floor area of 1500 ft^2 and a heat loss of 8 Btu/day °F ft^2 was assumed. The load-collector ratio (LCR) was then

$$LCR = 1500*8/AC \quad .$$

For buildings with different loads, the equivalent collector area would be

$$AC = LOAD/LCR \quad .$$

The solar savings fraction (SSF) is plotted as a function of collector area in Fig. 17a. The SSF is defined as

$$SSF = 1 - qaux/qd \quad .$$

Where, qd is the building heat loss if the room temperature was at 65°F. The nominal collector area in the remainder of the sensitivity studies was 250 ft^2. With this collector area, the solar savings fraction varies from 48.2% in Madison to 90.5% in Phoenix.

The energy utilized per year is plotted as a function of collector area in Fig. 17b. The energy utilized is defined as the energy delivered to the space minus the energy vented when the room temperature reached 75°F or

$$qu = qdel - qvt \quad .$$

At the nominal collector area of 250 ft^2, the energy utilized varies from 206,600 $Btu/ft_c^2/yr$ in Madison to 340,600 $Btu/ft_c^2/yr$ in Albuquerque.

The system efficiency is plotted as a function of collector area in Fig. 17c. The system efficiency is defined as the energy delivered divided by incident solar energy

$$eff = qdel/qinc \quad .$$

The efficiency is useful in comparing results with other systems and for evaluating the performance of a vapor system for other functions such as domestic water heating. The efficiency varies from 48.2% in Madison to 55.0% in Phoenix for the nominal collector area.

The results for the variation of collector tilt are given in Table IV and plotted in Figs. 18a-c. The curves show that the optimum angle is very flat, with the maximum solar savings fraction occurring at about 20 degrees greater than latitude and the maximum efficiency at about 10 degrees greater than latitude. Using the collector in a vertical position results in a performance decrease that varies from 18% in Madison to 5% in Phoenix. This peformance decrease would vary with collector area. However, a vertical collector on a space heating system does not produce an overheating problem in summer.

The effect on performance of varying the heat capacity of storage is given in Table V and Figs. 19a-c. As storage heat capacity is increased, the average operating temperature of the system is reduced and the system efficiency is increased. In addition, the room temperature swing is reduced and the amount of vented energy is decreased. An average storage heat capacity for an active solar energy system would be about 15 Btu/ft_c^2 °F. The performance increases about 20% if a storage heat capacity of 45 Btu/ft_c^2 °F is incorporated. We can realize a further performance increase averaging 9% when we increase the storage heat capacity to 105 Btu/ft^2 °F.

The sensitivity to the change in the storage heat loss coefficient is shown in Table VI and Figs. 20a-c. The results show that, beyond a value of 2.0 Btu/h ft_c^2 °F, there is very little change in performance. This is good because the true value of the parameter is uncertain. The nominal value of 4.0 Btu/h ft_c^2 °F (with a SCPM = 45 Btu/ft_c^2 °F) is about optimum for solar savings.

The last parameter investigated was the condenser heat transfer coefficient (UH) or the conductance between the vapor in the tubes of the condenser and water on the outside of the tubes. The results are shown in Table VII and Figs. 21a-c. With a self-pumping system, this coefficient controls the temperature difference and, hence, the pressure difference between the collector and the accumulator sides of the system. The condenser will automatically flood until the system can achieve the pressure difference required to push the condensate up to the accumulator. The experimental value of 7.0 Btu/h ft_c^2 °F obtained for the test cell is high up on the performance curve. For self-pumping systems with higher lift requirements, the value would automatically be lower even if the condenser area were larger because of the flooding of the condenser. A mechanically-pumped system could achieve the higher performance with the larger condenser coefficients because the condenser can be pumped dry. A coefficient of 20 Btu/h ft_c^2 °F would increase the SSF by an average of 4%, which could be achieved with a large condenser and a mechanical pump.

ACKNOWLEDGMENTS

Acknowledgments are due L. Dalton, J. Tafoya, and B. Ketchum, who designed, constructed, and instrumented the vapor system in the test cell. Jan Sander was responsible for the word processing and paper preparation, and Sherry Reisfeld was responsible for the editing.

REFERENCES

1. D. A. Neeper and R. D. McFarland, "Some Potential Benefits of Fundamental Research for the Passive Solar Heating and Cooling of Buildings," Los Alamos National Laboratory report LA-9425-MS (August 1982).

2. Joel Swisher, "Active Charge/Passive Discharge Solar Heating Systems: Thermal Analysis and Performance Comparisons," Solar Energy Research Institute report SERI/TR-721-1104 (June 1981).

3. J. C. Hedstrom, "Vapor-Phase Heat-Transport System," Passive and Hybrid Solar Energy Update Meeting, Washington, D.C., September 26-28, 1983. (Los Alamos National Laboratory report LA-UR-83-2646)

4. R. D. McFarland, "Passive Test Cell Data for the Solar Laboratory Winter 1980-81, Los Alamos National Laboratory report LA-9300-MS (May 1982).

5. R. D. McFarland, J. C. Hedstrom, J. D. Balcomb, and S. W. Moore, "Passive Test Cell Results for the 1981-82 Winter," Los Alamos National Laboratory Report LA-9543-MS (October 1982).

6. Ove Jorgensen, "Modelling and Simulation," International Energy Agency Task 1 Report, Thermal Insulation Laboratory. Technical University of Denmark (October 1978).

7. D. Curtis, T. Freeman, J. C. Hedstrom, T. Inooka, O. Jorgensen, M. Osumi, K. Hinotani, and P. Lermusieau, "Validation of Simulation Models Using Measured Performance Data from the Los Alamos Study Center," Los Alamos National Laboratory report LA-9028-MS (September 1981).

8. Ove Jorgensen, "Simulation Program Validation Using Domestic Hot Water System Data," International Energy Agency Task 1 Report," Thermal Insulation Laboratory. Technical Unuiversity of Denmark (August 1982).

9. J. C. Hedstrom, "Performance of a Solar Air Conditioning System Utilizing Boiling Collectors," Los Alamos National Laboratory report LA-9724-MS (April 1983).

NOMENCLATURE

AC	Collector area
ALF	Collector absorptivity
CL	Cell heat-loss coefficient to adjacent test cell
CM	Collector mass heat capacity
DD	Degree day
EC	Collector emissivity
EX	Glazing extinction coefficient
eff	System efficiency
GL	Number of glazings
ft_c^2	Square feet of collector
H	Collector heat-transfer coefficient between absorber and fluid
LOAD	Building heat-loss coefficient
LCR	Load collector ratio
qaux	Auxiliary heat
qcout	Collector heat output
qd	Building heat demand at TRNMIN
qdel	Heat delivered to building by solar energy system
qinc	Solar energy incident on collector
qu	Heat utilized by building
qvt	Heat vented when building reaches TRMMAX
SCPM	Storage mass heat capacity
SSF	Solar savings fraction
TC	Collector absorber temperature
TCOUT	Collector fluid outlet temperature
TS	Storage temperature
TRM	Room temperature
TRMMIN	Minumum room temperature
TRMMAX	Maximum room temperature
TILT	Collector tilt from horizontal
UB	Collector back heat-loss coefficient
UH	Condenser heat-transfer coefficient
UP1	Outside pipe heat-loss coefficient
UP2	Inside pipe heat-loss coefficient
US	Storage heat-loss coefficient
WCP	Collector flow rate

TABLE I

COMPARISON BETWEEN MEASURED AND CALCULATED DAILY ENERGY
CELL NO. 8

JDAY	SUN		AUX		MASS		COLL		LOAD	
	MEAS	CALC	MEAS	CALC	MEAS	CALC	MEAS	CALC	MEAS	CALC
1	1261	1261	657	700	36	131	519	556	1071	1125
2	901	901	908	829	-84	-69	220	312	1140	1209
3	1970	1970	848	731	218	343	722	943	1356	1330
4	1901	1901	413	348	182	180	888	919	890	1084
5	1919	1919	197	184	125	125	967	935	654	987
6	1914	1914	131	129	125	72	1012	927	734	977
7	1941	1941	86	86	37	20	993	917	978	977
8	1949	1949	81	117	-76	-3	925	917	1008	1031
9	1798	1798	144	181	-98	-76	889	842	1078	1094
10	1942	1942	223	260	-64	-42	966	887	1168	1187
11	1602	1602	366	368	-154	-179	700	655	1294	1201
13	1058	1058	798	675	-245	-180	217	398	1308	1253
15	1429	1429	1009	926	300	266	626	661	1411	1320
16	1986	1986	828	747	286	235	905	909	1511	1421
17	993	993	947	858	-305	-252	169	308	1452	1418
18	2076	2076	1007	972	283	251	901	924	1764	1645
19	1985	1985	851	742	167	101	872	890	1682	1531
20	2074	2074	624	596	87	62	943	918	1584	1451
21	1408	1400	747	710	-268	-225	468	534	1597	1469
22	1126	1126	875	817	-196	-173	303	379	1453	1368
23	1777	1777	816	761	212	171	804	795	1510	1385
24	2112	2112	559	538	243	229	1005	984	1417	1291
25	2079	2079	288	279	208	149	1104	1006	1240	1132
26	1667	1667	193	216	-123	-111	810	751	1155	1073
28	2092	2092	264	199	196	116	1045	1008	1165	1085
29	2145	2145	176	146	178	96	1126	1038	1155	1080
30	2128	2128	72	138	36	-38	1203	977	1260	1148
31	2112	2113	121	176	55	30	1172	1007	1329	1146
TOTAL	49345	49346	14229	13428	1361	1229	22474	22294	35365	34419
AVERAGE	1762	1762	508	480	49	44	803	796	1263	1229

TABLE II

COMPUTER MODEL INPUT PARAMETERS

Input Parameter		Validation Study	Sensitivity Study
LOAD	Btu/h °F	28.3	500
AC	ft^2	22.2	250
LCR	Btu/h ft_c^2 °F	1.28	2
TRMMIN	°F	65	65
TRMMAX	°F	95	75
TILT	degrees	36	LAT+20
WCP	Btu/h ft_c^2 °F	50	50
CL	Btu/h °F	0.16	0
ALF		0.90	0.90
EC		0.10	0.10
GL		1	1
EX	in-1	0.30	0.30
CM	Btu/ft_c^2 °F	1	1
UB	Btu/h ft_c^2 °F	0.3	0.3
H	Btu/h ft_c^2 °F	20	20
SCPM	Btu/ft_c^2 °F	45	45
US	Btu/h ft_c^2 °F	1.5	4
UH	Btu/h ft_c^2 °F	7	7
UP1	Btu/h ft_c^2 °F	0.05	0.05
UP2	Btu/h ft_c^2 °F	0.60	0.10

TABLE III

SENSITIVITY TO COLLECTOR AREA

Albuquerque, New Mexico

ac	qinc	qcout	qdel	qsl	qaux	qd	qld	qvt	qpipe	SSF	eff
50	709625	397232	390455	380362	921710	1148020	1309075	3078	10206	19.7	55.0
100	709625	392313	386331	376444	366923	574010	746065	6031	9999	36.1	54.3
150	709625	387267	380058	370324	192263	382635	540500	11609	9847	49.8	53.6
200	709625	382329	374889	366260	112157	287006	467247	19556	9741	60.9	52.8
250	709625	377632	369964	360408	68643	229604	408017	29339	9667	70.1	52.1
300	709625	373326	365449	355944	42703	191375	367752	40147	9611	77.7	51.5
400	709625	365622	357386	347919	16808	143502	310782	63149	9534	88.3	50.4
500	709625	359038	350832	341052	6877	114802	272040	85061	9461	94.0	49.4

Madison, Wisconsin

ac	qinc	qcout	qdel	qsl	qaux	qd	qld	qvt	qpipe	SSF	eff
50	435594	226428	220864	215361	1672576	1816350	1894364	27	5670	7.9	50.7
100	435594	223000	218327	212931	773178	906175	991677	210	5663	14.5	50.1
150	435594	220341	215548	210241	478287	605389	693427	565	5474	21.0	49.5
200	435594	217561	212652	207427	333871	454088	545152	1445	5392	26.5	48.8
250	435594	214801	209782	204628	249227	363270	455858	3192	5321	31.4	48.2
300	435594	212384	207252	202149	193960	302786	395608	5627	5270	35.9	47.6
400	435594	207832	202545	197549	127220	227044	317869	11895	5163	44.0	46.5
500	435594	204071	198641	193716	89470	181635	268962	19142	5092	50.7	45.6

Washington, D.C.

ac	qinc	qcout	qdel	qsl	qaux	qd	qld	qvt	qpipe	SSF	eff
50	443074	241879	237770	231928	1065388	1200990	1304842	165	5916	11.3	53.7
100	443074	238852	234612	228857	474029	600495	708651	635	5830	21.1	53.0
150	443074	235763	231394	225726	281972	400290	511748	1840	5742	29.6	52.2
200	443074	232705	228213	222625	188814	300247	413226	3866	5661	37.1	51.5
250	443074	229786	225167	219639	134635	240198	353404	6577	5597	43.9	50.8
300	443074	226945	222224	216744	100496	200205	312605	10041	5535	49.8	50.2
400	443074	221786	216869	211423	61024	150124	259288	18437	5449	59.4	48.9
500	443074	217672	212591	207123	39802	120099	224597	27530	5390	66.9	48.0

Phoenix, Arizona

ac	qinc	qcout	qdel	qsl	qaux	qd	qld	qvt	qpipe	SSF	eff
50	703976	414017	408373	397863	280678	411000	630942	57807	10484	31.7	58.0
100	703976	408024	402108	391632	92213	205500	419689	74262	10445	56.1	57.1
150	703976	402775	396604	386105	37692	136986	342861	91029	10438	72.5	56.3
200	703976	398015	391612	381075	16403	102750	300053	107538	10443	84.0	55.6
250	703976	393545	386935	376356	7775	82200	271363	122904	10442	90.5	55.0
300	703976	389581	382782	372151	4144	68514	249134	137330	10444	94.0	54.4
400	703976	383571	376514	365806	1294	51375	213126	164188	10432	97.5	53.5
500	703976	379482	372294	361504	368	41100	183626	188509	10428	99.1	52.9

Denver, Colorado

ac	qinc	qcout	qdel	qsl	qaux	qd	qld	qvt	qpipe	SSF	eff
50	639009	350708	344446	335350	1324801	1569960	1669718	186	8986	15.6	53.9
100	639009	347667	341245	332353	555432	784980	895646	923	8821	29.2	53.4
150	639009	344129	337544	328805	309013	523268	643237	3026	8656	40.9	52.8
200	639009	340415	333657	325022	192108	392490	518928	6454	8520	51.1	52.2
250	639009	336589	329659	321095	126342	313992	444663	10884	8408	59.8	51.6
300	639009	332882	325771	317234	85634	261712	394684	16193	8325	67.3	51.0
400	639009	325758	318347	309817	41316	196245	329741	29261	8191	78.9	49.8
500	639009	319217	311560	302999	20817	156996	288266	43331	8088	86.7	48.8

UNITS: ac-ft^2; energy-Btu/ft^2 yr; SSF-%; eff-%

TABLE IV

SENSITIVITY TO COLLECTOR TILT

Albuquerque, New Mexico

tilt	qinc	qcout	qdel	qsl	qaux	qd	qld	qvt	qpipe	SSF	eff
0	671339	331685	324828	316258	122518	229604	393762	53567	8775	46.6	48.4
15	734977	378696	370868	361084	98297	229604	409683	57372	9976	48.1	50.5
30	759724	399735	391658	381362	79441	229604	418080	52868	10446	48.4	51.6
45	743179	396082	387105	377022	70609	229604	416817	40668	10205	49.2	52.1
60	687234	364794	357373	348199	60881	229604	402637	23364	9282	70.0	52.0
75	596385	310789	304448	296888	74606	229604	377783	6954	7704	67.6	51.0
90	478397	241004	236133	230488	90328	229604	326169	630	5786	60.7	49.4

Madison, Wisconsin

tilt	qinc	qcout	qdel	qsl	qaux	qd	qld	qvt	qpipe	SSF	eff
0	433338	192109	187626	183018	287094	363270	464065	10836	4914	21.0	43.3
15	470637	220740	215637	210148	268542	363270	471693	12490	6644	26.1	46.8
30	485391	238217	229730	223959	255676	363270	473723	11736	5984	29.6	47.3
45	476700	234904	229444	223705	248964	363270	469927	8611	6925	31.6	48.1
60	444868	219565	214446	209158	248538	363270	458980	4031	5457	31.6	48.2
75	393060	191248	186741	182243	254656	363270	440731	758	4665	29.9	47.5
90	324543	151128	147548	144154	268679	363270	416670	36	3573	26.0	45.5

Washington, D.C.

tilt	qinc	qcout	qdel	qsl	qaux	qd	qld	qvt	qpipe	SSF	eff
0	42819	212368	207957	202886	165686	240198	358154	15704	5333	31.0	47.0
15	476822	237971	233077	227281	150313	240198	366139	17354	5983	37.4	48.9
30	487585	249588	244514	238406	140020	240198	368520	16023	6240	41.7	50.1
45	475110	245950	241003	235020	134958	240198	364253	11683	6072	43.8	50.7
60	439951	228104	223520	218040	135007	240198	352303	6209	5549	43.8	50.8
75	385187	196967	193046	188430	140591	240198	331934	1824	4685	41.5	50.1
90	314771	155440	152398	148914	152664	240198	305938	162	3579	36.4	48.4

Phoenix, Arizona

tilt	qinc	qcout	qdel	qsl	qaux	qd	qld	qvt	qpipe	SSF	eff
0	683327	367247	361229	351374	22289	82200	228675	154795	10032	72.9	52.9
15	740027	408386	401591	390512	13734	82200	250245	164878	11138	83.3	54.3
30	757569	423584	416483	404955	9620	82200	265521	160264	11483	88.3	55.0
45	734309	411111	404211	393087	8060	82200	271979	139880	11008	90.2	55.0
60	672702	374285	367996	358009	7787	82200	268346	106982	9843	90.5	54.7
75	577247	315626	310370	302189	8624	82200	251808	66740	8052	89.5	53.8
90	457376	243933	240086	234117	11436	82200	218665	32619	5906	86.1	52.5

Denver, Colorado

tilt	qinc	qcout	qdel	qsl	qaux	qd	qld	qvt	qpipe	SSF	eff
0	580436	274601	268553	261667	195584	313992	440701	23441	7112	37.7	46.3
15	648360	324141	317250	308984	163826	313992	483890	27038	8576	47.9	48.9
30	681567	351705	344364	335336	141346	313992	489825	25821	9021	55.0	50.5
45	677704	354942	347628	338546	129192	313992	487395	19026	8982	58.9	51.3
60	637130	336618	328704	320167	126383	313992	444026	10607	8380	59.7	51.6
75	564353	293927	287867	280601	133043	313992	417744	3059	7203	57.5	51.0
90	464279	233137	228379	222715	152662	313992	391498	49	5548	51.4	49.2

UNITS: tilt-degree; energy-Btu/ft^2 yr; SSF-%; eff-%

TABLE V

SENSITIVITY TO STORAGE HEAT CAPACITY

Albuquerque, New Mexico

scpm	qinc	qcout	qdel	qsl	qaux	qd	qld	qvt	qpipe	SSF	eff
15	743065	339892	329632	314124	98119	229604	386410	38607	10354	88.6	44.3
30	743065	379656	370986	369345	78440	229604	407692	41337	11668	85.8	49.9
45	743065	398023	387047	376965	70893	229604	416794	40614	10903	89.3	52.1
60	743065	403120	396503	386293	65469	229604	421833	39680	9433	71.4	53.2
75	743065	408084	400691	392063	62184	229604	424445	38493	8965	72.9	53.9
90	743065	411476	404227	396024	59467	229604	426309	37586	8636	74.1	54.4
105	743065	413913	406780	398920	57286	229604	427617	36781	8400	75.1	54.7

Madison, Wisconsin

scpm	qinc	qcout	qdel	qsl	qaux	qd	qld	qvt	qpipe	SSF	eff
15	435594	188164	179883	171834	267230	363270	441564	5266	8021	26.4	41.3
30	435594	206692	201314	195312	255008	363270	451990	4212	6067	29.8	46.2
45	435594	214801	209782	204628	249227	363270	455858	3192	5321	31.4	48.2
60	435594	219095	214278	209616	245613	363270	457642	2452	4935	32.4	49.2
75	435594	221743	217076	212756	242933	363270	458515	1878	4701	33.1	49.8
90	435594	223569	218977	214923	240939	363270	459007	1486	4543	33.7	50.3
105	435594	224904	220375	216539	239331	363270	459322	1166	4432	34.1	50.6

Washington, D.C.

scpm	qinc	qcout	qdel	qsl	qaux	qd	qld	qvt	qpipe	SSF	eff
15	443074	198992	192974	184400	153368	240198	336448	9504	8475	36.1	43.6
30	443074	221288	216293	209898	140915	240198	348902	8096	6369	41.3	48.8
45	443074	229786	226167	219639	134835	240198	353404	6577	5697	43.9	50.3
60	443074	234187	229786	224762	131030	240198	355524	5483	5195	45.4	51.9
75	443074	236949	232676	227995	128413	240198	356864	4649	4957	46.5	52.5
90	443074	238817	234633	230217	126424	240198	357757	3985	4798	47.4	53.0
105	443074	240175	236056	231860	124922	240198	358464	3469	4686	48.0	53.3

Phoenix, Arizona

scpm	qinc	qcout	qdel	qsl	qaux	qd	qld	qvt	qpipe	SSF	eff
15	703976	338113	328848	312670	18116	82200	240808	105447	15943	78.0	46.7
30	703976	378191	370820	358603	10631	82200	261935	118939	12012	87.1	52.7
45	703976	393645	386938	376356	7775	82200	271363	122904	10442	90.5	55.0
60	703976	401683	395369	385699	6452	82200	276855	124452	9614	92.4	56.2
75	703976	406468	400501	391433	5382	82200	280564	125129	9099	93.5	56.9
90	703976	409765	403961	396340	4786	82200	283260	125420	8750	94.2	57.4
105	703976	412102	406426	398155	4270	82200	285218	125527	8494	94.8	57.7

Denver, Colorado

scpm	qinc	qcout	qdel	qsl	qaux	qd	qld	qvt	qpipe	SSF	eff
15	639009	290012	280985	267975	157894	313992	423778	14427	12758	49.7	44.0
30	639009	323584	316060	306214	136432	313992	439199	12703	9613	56.5	49.5
45	639009	336889	329659	321095	126342	313992	444663	10884	8408	59.8	51.6
60	639009	343569	336067	329093	119852	313992	446943	9541	7790	61.8	52.7
75	639009	347893	341483	334084	115230	313992	447988	8530	7416	63.3	53.4
90	639009	350868	344596	337539	111752	313992	448535	7751	7168	64.4	53.9
105	639009	352983	346821	340044	109069	313992	448859	7111	6987	65.3	54.3

UNITS: scpm-Btu/ft^2 °F; energy-Btu/ft^2 yr; SSF-%; eff-%

TABLE VI

SENSITIVITY TO STORAGE HEAT LOSS COEFFICIENT

Albuquerque, New Mexico

us	qinc	qcout	qdel	qsl	qaux	qd	qld	qvt	qpipe	SSF	eff
0.5	743055	284031	272696	252524	99720	229604	355346	15158	18509	56.6	36.7
1.0	743055	336509	326344	310239	82447	229604	384993	22718	15305	64.1	43.9
1.5	743055	369838	350436	336596	76994	229604	398164	27603	13416	66.9	47.2
2.0	743055	372951	364069	351624	72994	229604	408394	31181	12231	68.2	49.0
3.0	743055	387308	379005	368095	70809	229604	412977	35816	10918	69.2	51.0
4.0	743055	395023	387047	376965	70593	229604	416794	40614	10203	69.3	52.1
5.0	743055	399813	392031	382467	71099	229604	419013	43934	9765	69.0	52.8
8.0	743055	407610	400127	391341	73340	229604	422021	51322	9080	68.1	53.8

Madison, Wisconsin

us	qinc	qcout	qdel	qsl	qaux	qd	qld	qvt	qpipe	SSF	eff
0.5	435594	161396	155063	145510	269981	363270	423748	729	9112	25.7	35.6
1.0	435594	186690	180875	173182	258669	363270	437972	1287	7636	28.8	41.5
1.5	435594	198229	192644	185838	253945	363270	444709	1699	6760	30.1	44.2
2.0	435594	204430	199067	192871	251668	363270	448582	2041	6217	30.7	45.7
3.0	435594	211267	206117	200581	249751	363270	453198	2648	5644	31.2	47.3
4.0	435594	214801	209782	204628	249227	363270	455858	3192	5321	31.4	48.2
5.0	435594	217063	212126	207213	249303	363270	457820	3695	5126	31.4	48.7
8.0	435594	220441	215637	211123	250461	363270	461377	4883	4812	31.1	49.5

Washington, D.C.

us	qinc	qcout	qdel	qsl	qaux	qd	qld	qvt	qpipe	SSF	eff
0.5	443074	172396	166041	154848	155765	240198	316551	2545	9895	35.7	37.5
1.0	443074	199611	193946	185134	143084	240198	332579	3587	8088	40.4	43.8
1.5	443074	211669	206413	198861	138548	240198	340117	4255	7116	42.3	46.6
2.0	443074	218454	213433	206621	136361	240198	344597	4753	6555	43.2	48.2
3.0	443074	225806	221060	215092	134877	240198	350068	5707	5924	43.8	49.9
4.0	443074	229786	225167	219639	134835	240198	353404	6577	5597	43.9	50.8
5.0	443074	232174	227651	222406	135267	240198	355646	7352	5388	43.7	51.4
8.0	443074	235760	231369	226562	137201	240198	359641	9188	5064	42.9	52.2

Phoenix, Arizona

us	qinc	qcout	qdel	qsl	qaux	qd	qld	qvt	qpipe	SSF	eff
0.5	703976	280333	269806	249076	17885	82200	221872	63859	19007	78.2	38.3
1.0	703976	333514	324356	307710	11262	82200	247463	87018	15758	86.3	46.1
1.5	703976	357204	348970	334660	9075	82200	258272	98952	13748	89.0	49.6
2.0	703976	370664	362994	350028	8224	82200	264086	106474	12575	90.0	51.6
3.0	703976	385501	378506	367087	7771	82200	269479	116290	11196	90.5	53.8
4.0	703976	393645	386930	376356	7775	82200	271363	122904	10442	90.5	55.0
5.0	703976	398749	392262	382280	7903	82200	271753	128105	9997	90.4	55.7
8.0	703976	407259	401270	391977	8423	82200	270232	139094	9285	89.8	57.0

Denver, Colorado

us	qinc	qcout	qdel	qsl	qaux	qd	qld	qvt	qpipe	SSF	eff
0.5	639009	246291	236557	218939	164516	313992	394162	4856	15422	47.6	37.0
1.0	639009	289371	280746	267005	142357	313992	415270	6387	12602	54.7	43.9
1.5	639009	308486	300446	288655	133622	313992	425575	7464	10984	57.4	47.0
2.0	639009	319220	311584	300984	129501	313992	431990	8292	10037	58.8	48.8
3.0	639009	330677	323492	314209	126525	313992	438777	9672	8986	59.7	50.6
4.0	639009	336589	329659	321095	126342	313992	444663	10884	8408	59.8	51.6
5.0	639009	340201	333422	325298	127121	313992	448208	11945	8053	59.5	52.2
8.0	639009	345427	338888	331448	130843	313992	454933	14493	7498	58.3	53.0

UNITS: us-Btu/h ft^2 °F; energy-Btu/ft^2 yr; SSF-%; eff-%

TABLE VII

SENSITIVITY TO CONDENSER HEAT TRANSFER COEFFICIENT

Albuquerque, New Mexico

uh	qinc	qcout	qdel	qsl	qaux	qd	qld	qvt	qpipe	SSF	eff
1	709625	243806	228180	201846	112367	229604	338404	4608	26540	50.8	32.2
2	709625	308639	296676	278106	89307	229604	372472	13274	18630	61.1	41.8
3	709625	337729	327825	312739	80046	229604	388164	19220	14925	66.1	46.2
4	709625	354228	348061	332416	75142	229604	396859	23128	12772	67.3	48.6
5	709625	364826	356347	345095	72136	229604	402401	25851	11371	68.6	50.2
7	709625	377632	369964	360408	68643	229604	409017	29339	9667	70.1	52.1
10	709625	387678	380657	372449	65989	229604	414125	32256	8311	71.3	53.6
20	709625	399066	393625	387063	62869	229604	420236	35977	6657	72.6	55.5

Madison, Wisconsin

uh	qinc	qcout	qdel	qsl	qaux	qd	qld	qvt	qpipe	SSF	eff
1	435594	138851	130141	116228	286208	363270	415611	144	15154	21.5	29.9
2	435594	176191	168667	158361	267253	363270	435347	726	10511	26.4	38.7
3	435594	192570	186084	177921	259528	363270	444217	1489	8352	28.6	42.7
4	435594	201803	195922	188992	255235	363270	449129	2098	7110	29.7	45.0
5	435594	207638	202158	196036	252491	363270	452152	2554	6296	30.5	46.4
7	435594	214801	209782	204628	249227	363270	456858	3192	5321	31.4	48.2
10	435594	220439	215796	211418	246666	363270	458744	3745	4540	32.1	49.5
20	435594	227221	223049	219630	243621	363270	462213	4470	3574	32.9	51.2

Washington, D.C.

uh	qinc	qcout	qdel	qsl	qaux	qd	qld	qvt	qpipe	SSF	eff
1	443074	149953	140317	124338	166815	240198	307328	424	16166	30.6	31.7
2	443074	188713	181397	170346	150649	240198	329852	2284	11186	37.3	40.9
3	443074	206162	199950	191191	143691	240198	339922	3809	8869	40.2	44.1
4	443074	215925	210370	202939	139989	240198	345547	4852	7523	41.7	47.5
5	443074	222204	217072	210499	137635	240198	349141	5577	6654	42.7	49.0
7	443074	229786	225167	219639	134835	240198	353404	6577	5597	43.9	50.8
10	443074	235678	231478	226786	132671	240198	356687	7420	4750	44.8	52.2
20	443074	242881	239172	235497	130094	240198	360659	8539	3721	45.8	54.0

Phoenix, Arizona

uh	qinc	qcout	qdel	qsl	qaux	qd	qld	qvt	qpipe	SSF	eff
1	703976	253806	239019	211435	19413	82200	206664	51613	27687	76.4	34.0
2	703976	321670	310665	291027	12030	82200	239480	82909	19622	85.4	44.1
3	703976	352119	342910	327023	9831	82200	253345	99038	15826	88.0	48.7
4	703976	369348	361196	347475	8856	82200	261005	108654	13628	89.2	51.3
5	703976	380351	372887	360576	8321	82200	265768	115035	12198	89.9	53.0
7	703976	393545	386935	376356	7775	82200	271363	122904	10442	90.5	55.0
10	703976	403944	398003	388796	7363	82200	275691	129213	9049	91.0	56.5
20	703976	416441	411327	403803	6892	82200	280745	136980	7338	91.6	58.4

Denver, Colorado

uh	qinc	qcout	qdel	qsl	qaux	qd	qld	qvt	qpipe	SSF	eff
1	639009	217006	202929	179472	182812	313992	385069	697	23564	41.8	31.8
2	639009	274974	264174	247688	163512	313992	413494	3960	16475	51.1	41.3
3	639009	301008	291795	278693	141524	313992	426577	6425	13135	54.9	45.7
4	639009	315774	307507	296211	135045	313992	434066	8109	11194	57.0	48.1
5	639009	325226	317552	307481	131039	313992	438872	9308	9945	58.3	49.7
7	639009	336589	329659	321095	126342	313992	444663	10884	8408	59.8	51.6
10	639009	345576	339226	331855	122706	313992	449234	12210	7191	60.9	53.1
20	639009	356425	350774	344865	118431	313992	454727	13948	5697	62.3	54.9

UNITS: uh-Btu/h ft^2 °F; energy-Btu/ft^2 yr; SSF-%; eff-%

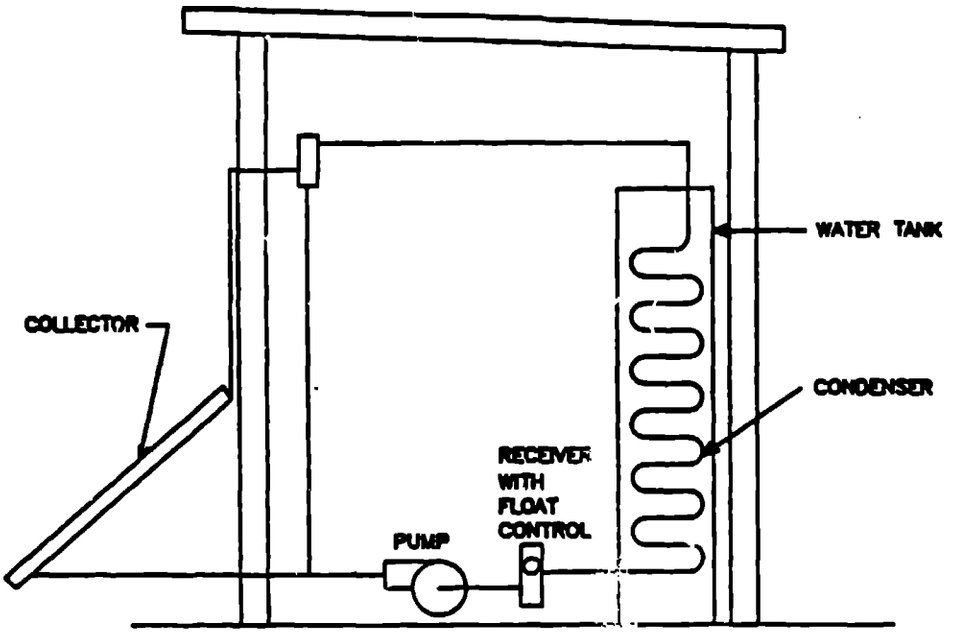

Fig. 1. Schematic of vapor-transport test cell with mechanical pump.

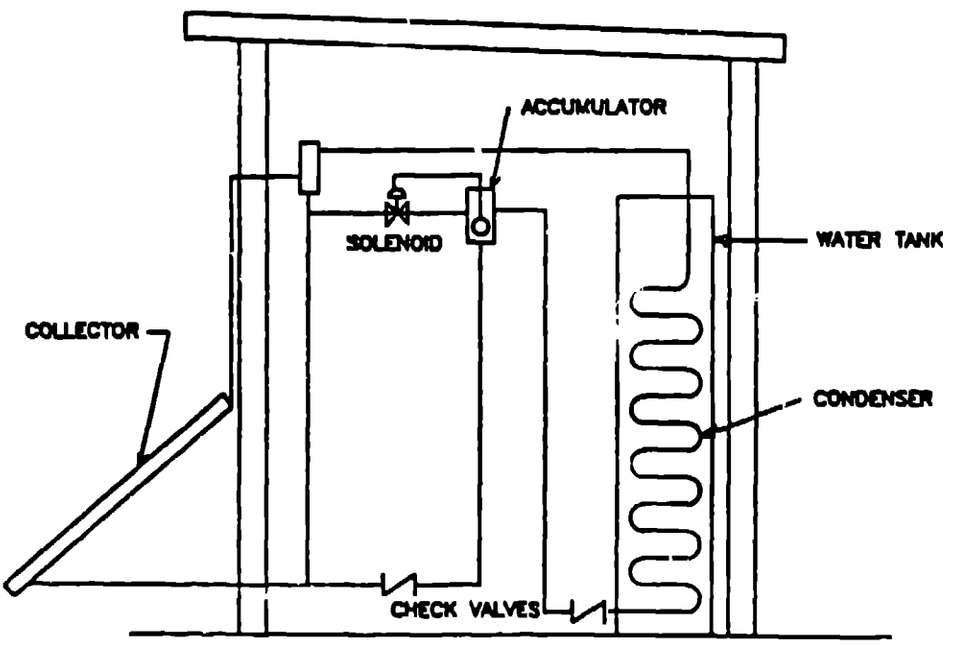

Fig. 2. Schematic of vapor-transport test cell with self-pumping condensate return.

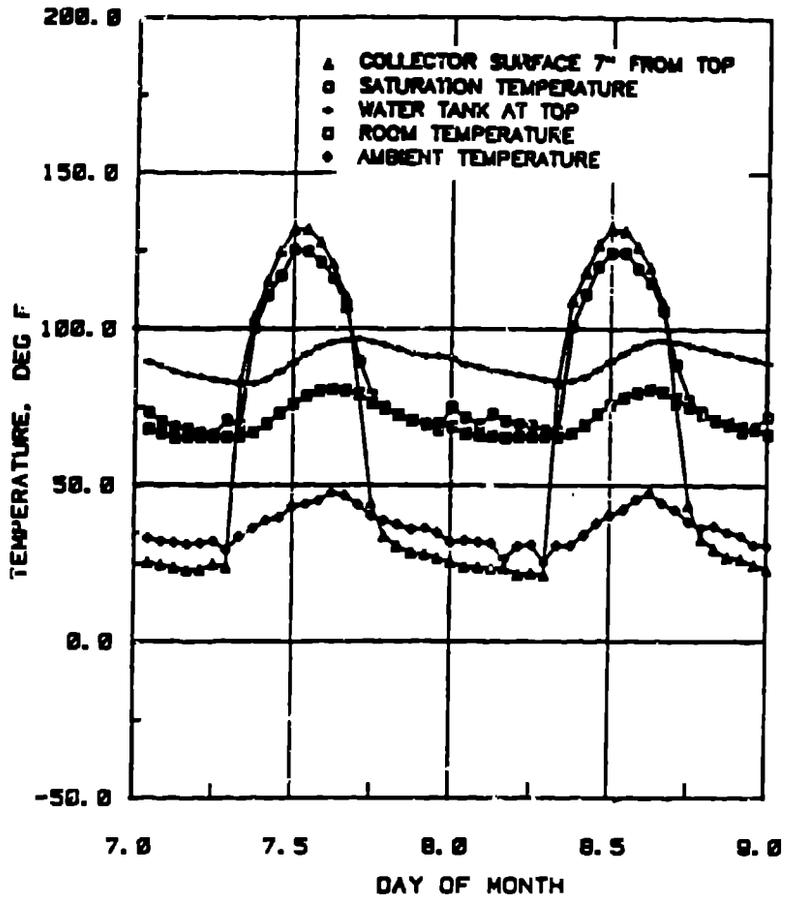

Fig. 3. Temperatures obtained from vapor-transport test cell on January 7-8, 1984. System is in self-pumping mode.

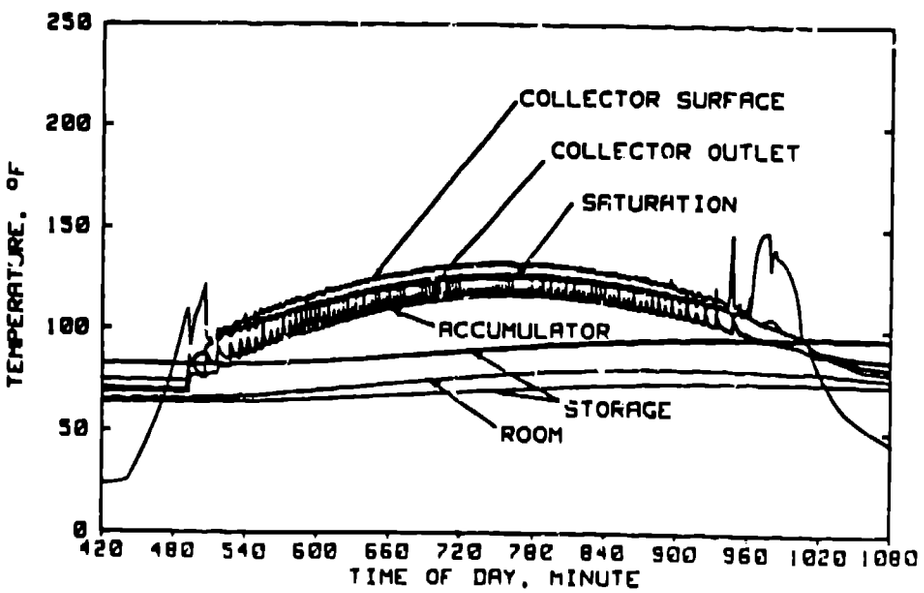

Fig. 4. Detailed temperature data obtained from vapor-transport test cell on January 7, 1984.

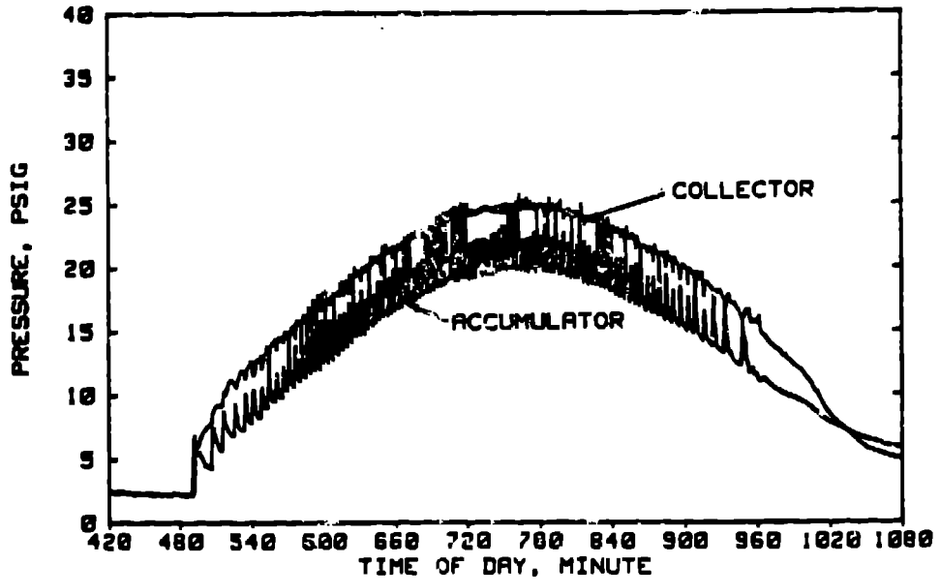

Fig. 5. Detailed pressure data obtained from vapor-transport test cell on January 7, 1984. System is in self-pumping mode.

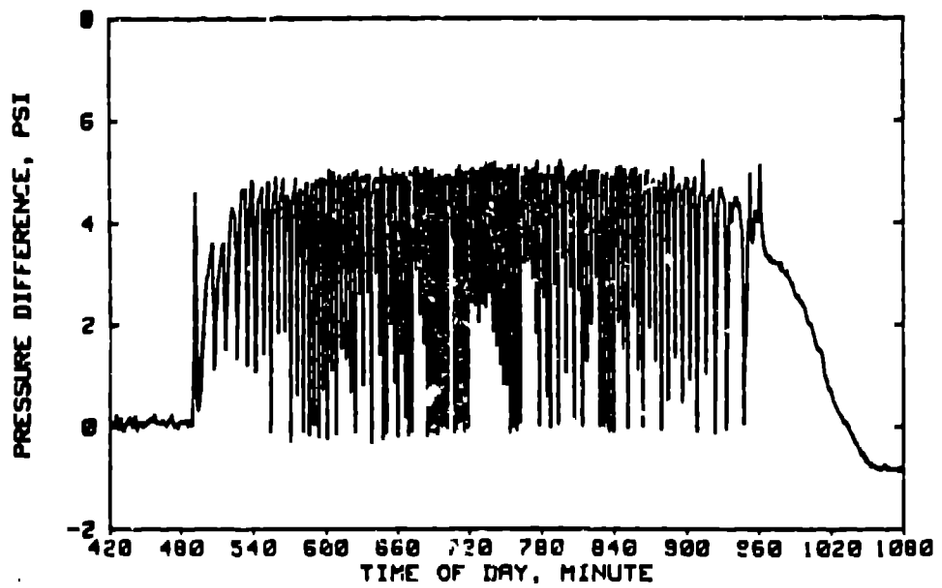

Fig. 6. Pressure difference between the collector and the accumulator, January 7, 1984. System is in self-pumping mode.

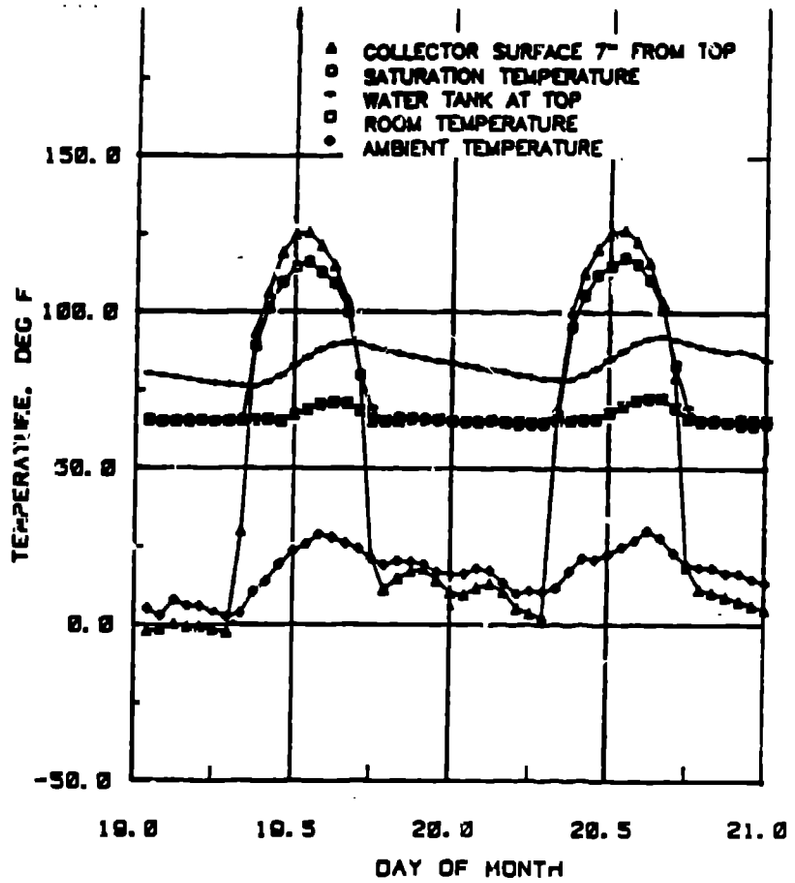

Fig. 7. Temperatures obtained from vapor-transport test cell on January 19-20, 1984. The pump is returning the liquid back to the collector.

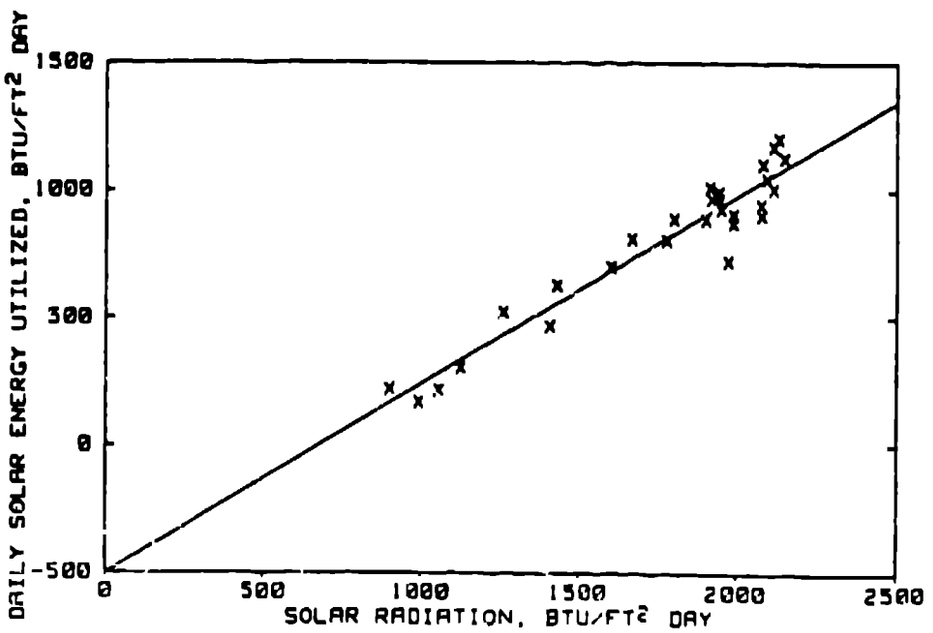

Fig. 8. Daily performance of the vapor system in Test Cell 8 for January 1984.

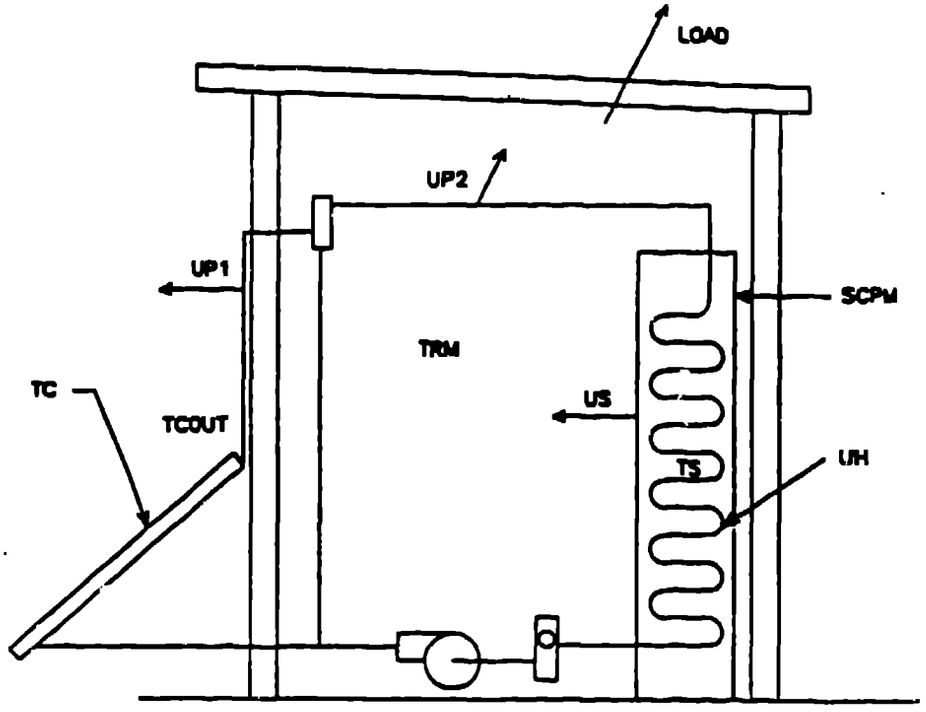

Fig. 9. Computer model of vapor-transport system.

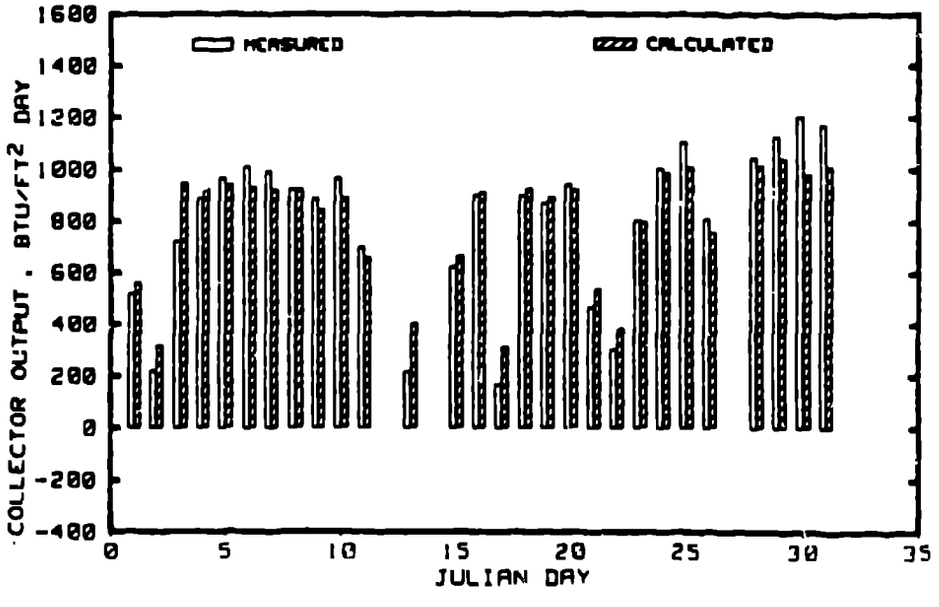

Fig. 10. Daily comparison of measured and predicted collector output from Test Cell 8.

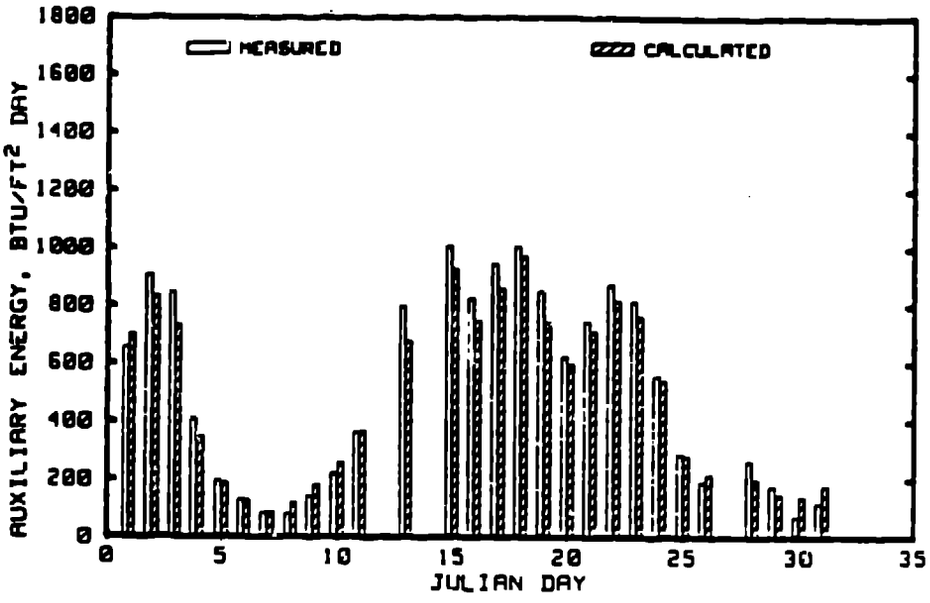

Fig. 11. Daily comparison of measured and predicted auxiliary energy from Test Cell 8.

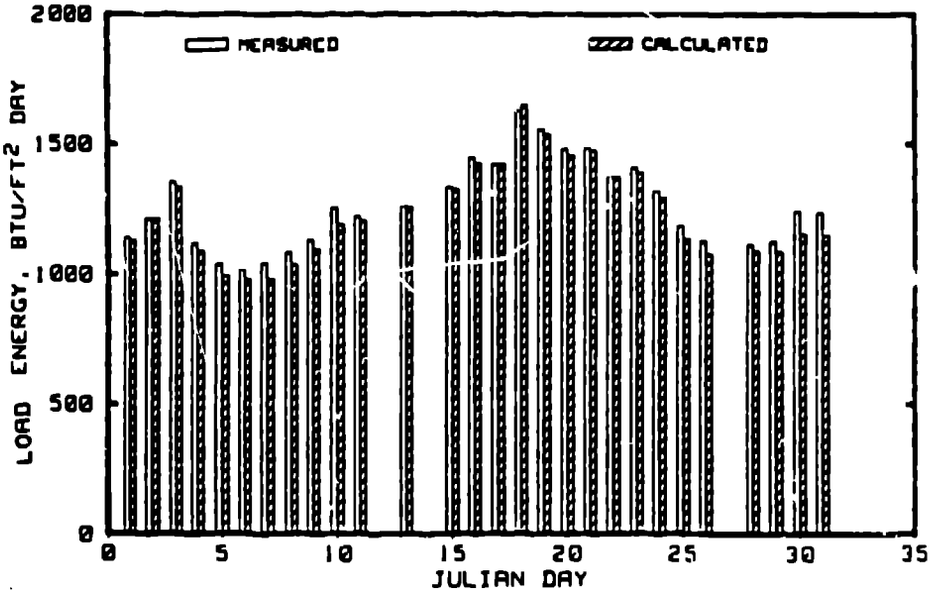

Fig. 12. Daily comparison of measured and predicted load from Test Cell 8.

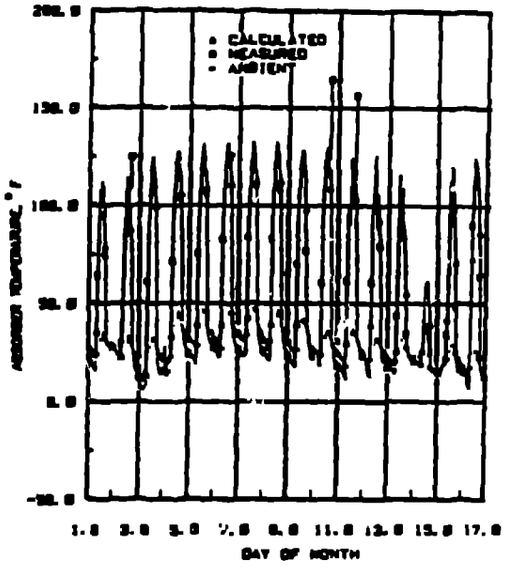

13.a.

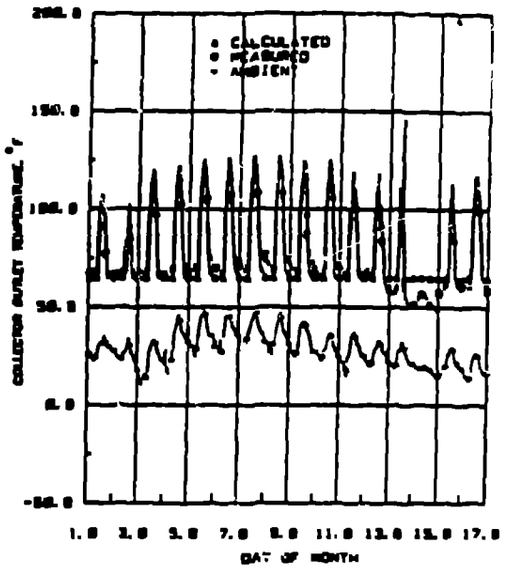

13.b.

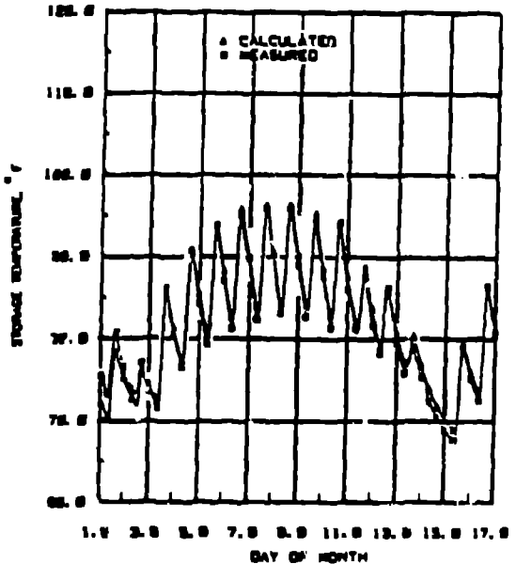

13.c.

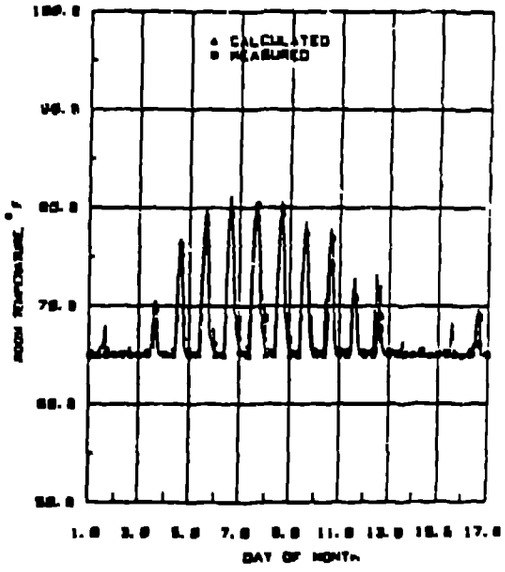

13.d.

Fig. 13a-d. Hourly comparison of measured and predicted temperatures from Test Cell 8 for January 1-16, 1984.

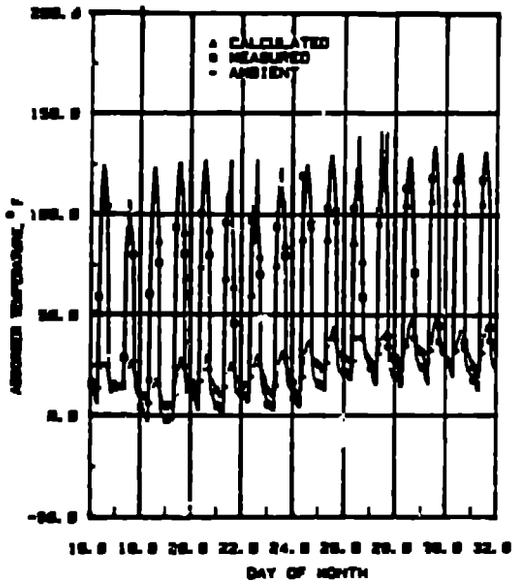

14.a.

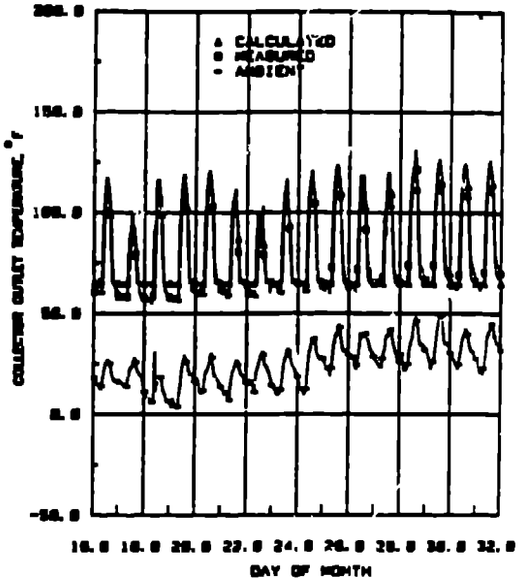

14.b.

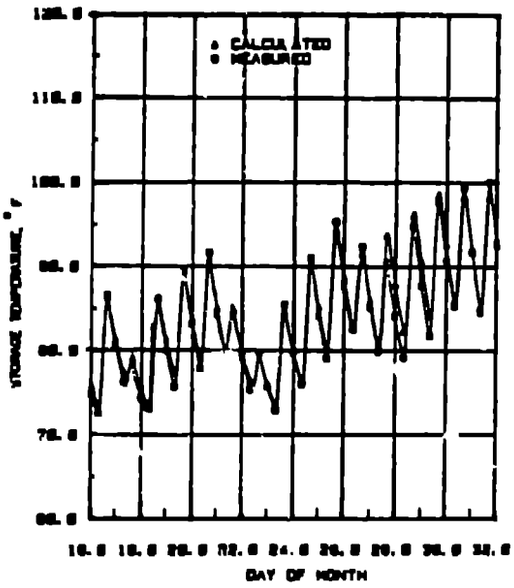

14.c.

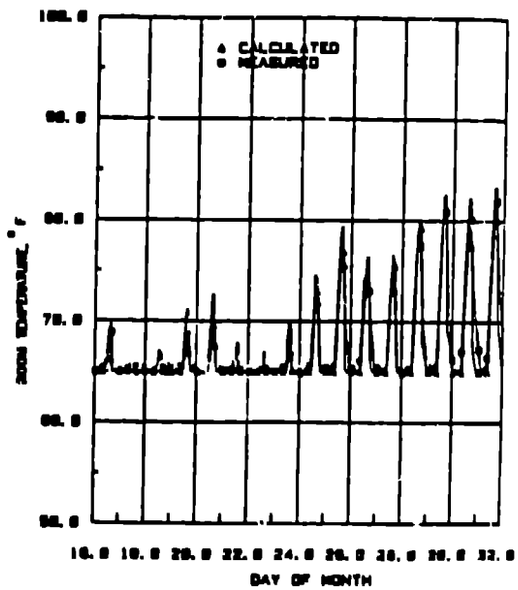

14.d.

Fig. 14a-d. Hourly comparison of measured and predicted temperatures from Test Cell 8 for January 16-31, 1984.

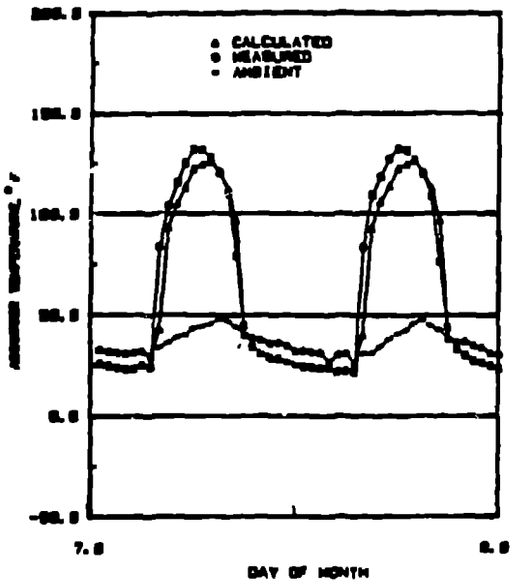

15.a.

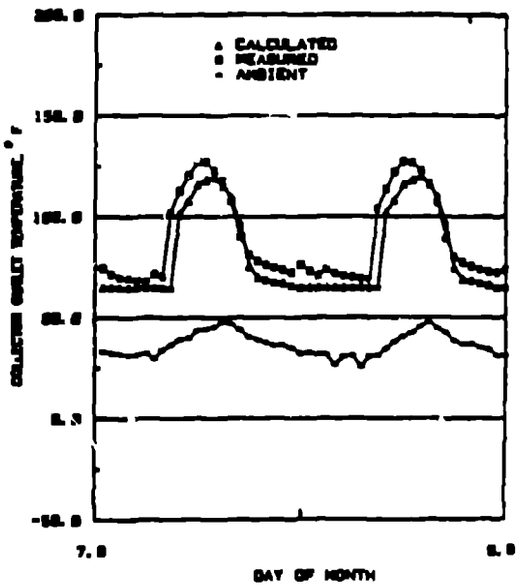

15.b.

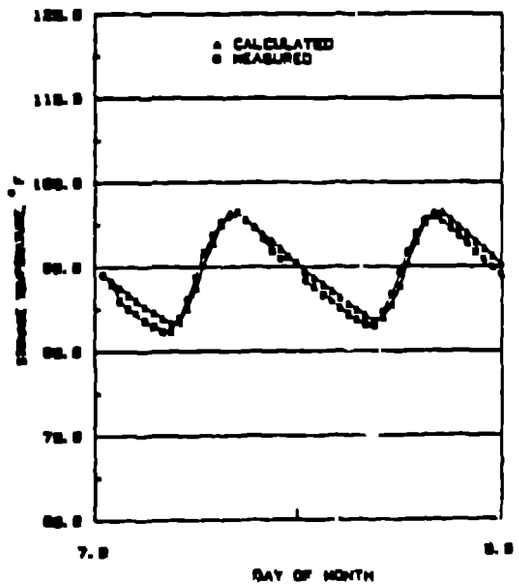

15.c.

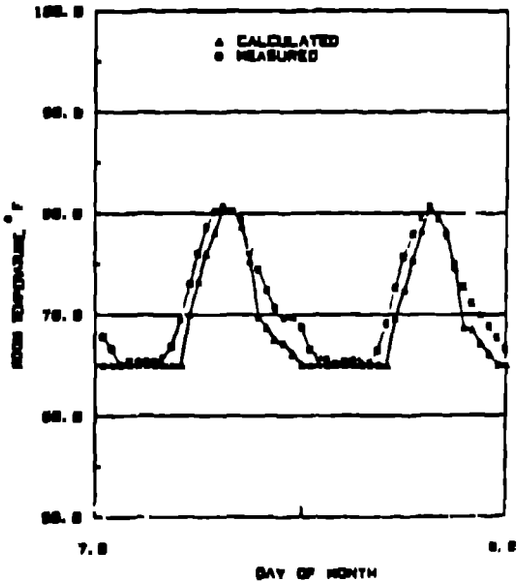

15.d.

Fig. 15a-d. Hourly comparison of measured and predicted temperatures from Test Cell 8 for January 7-8, 1984.

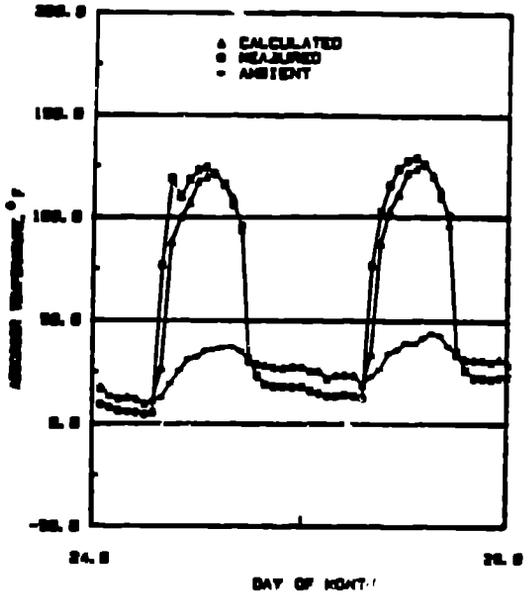

16.a.

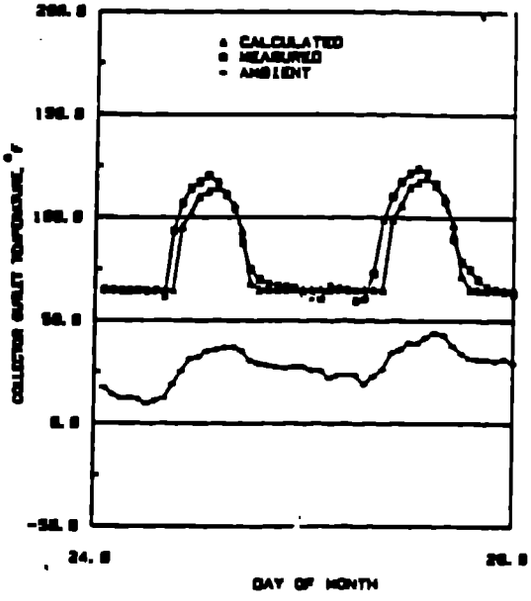

16.b.

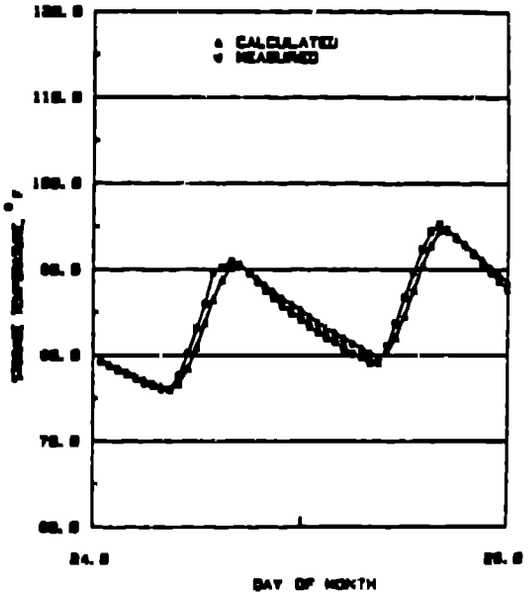

16.c.

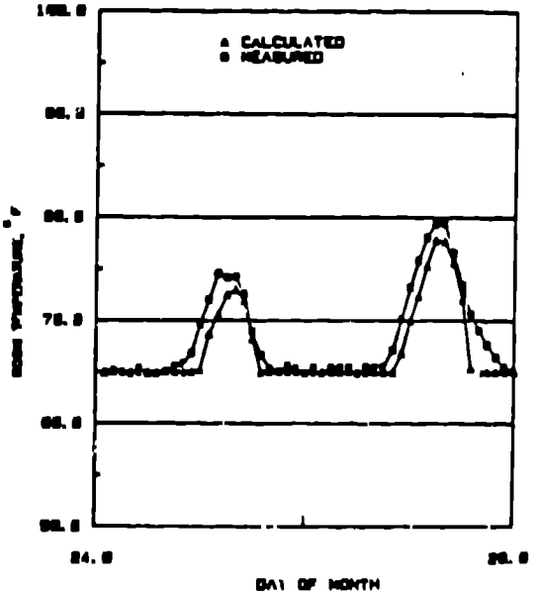

16.d.

Fig. 16a-d. Hourly comparison of measured and predicted temperatures from Test Cell 8 for January 24-25, 1984.

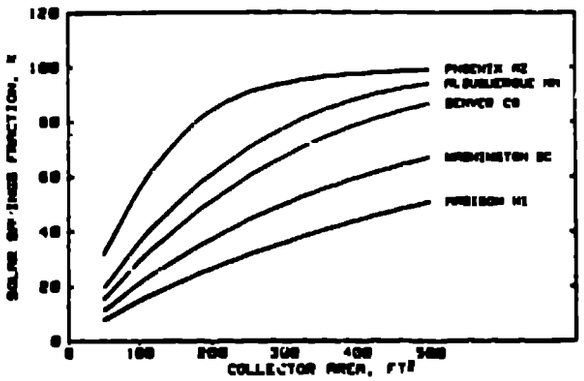

17.a.

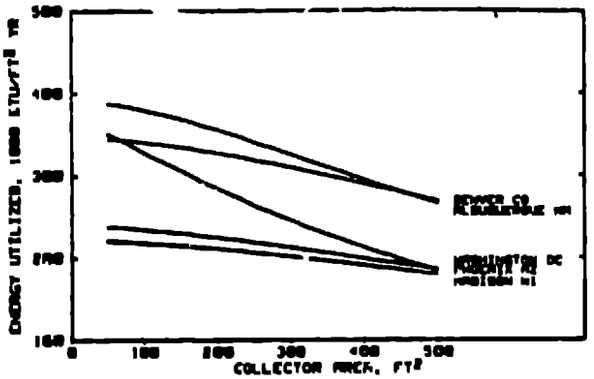

17.b.

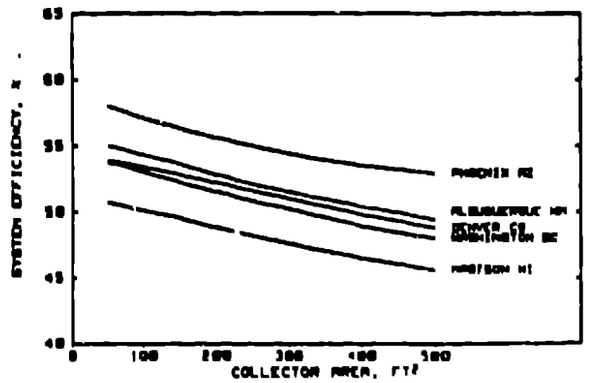

17.c.

Fig. 17a-c. System performance factors for five cities as a function of collector area. Building load is 12,000 Btu/day °F.

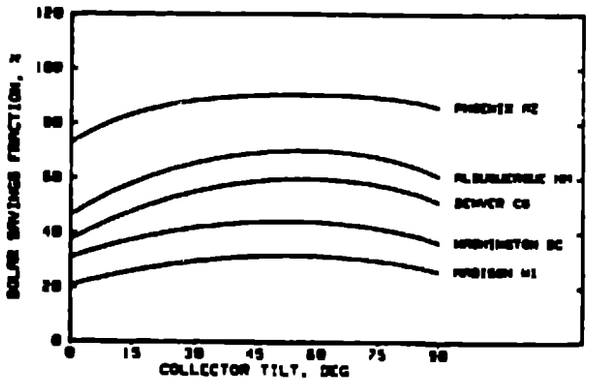

18.a.

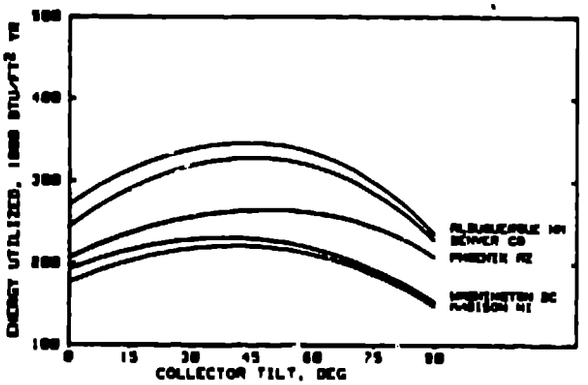

18.b.

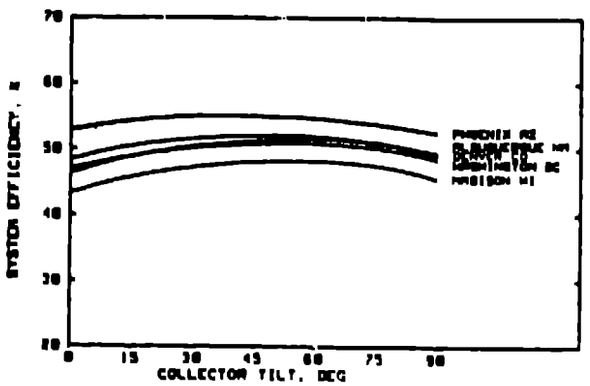

18.c.

Fig. 18a-c. System performance factors for five cities as a function of collector tilt.

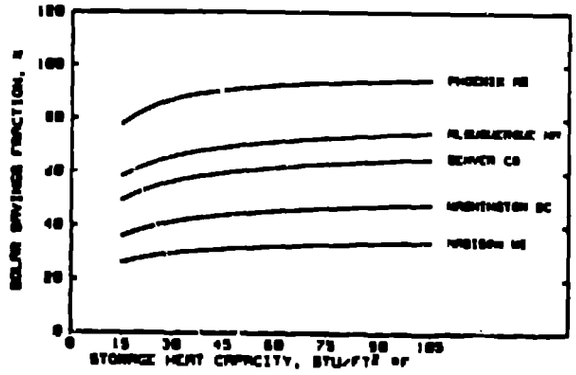

19.a.

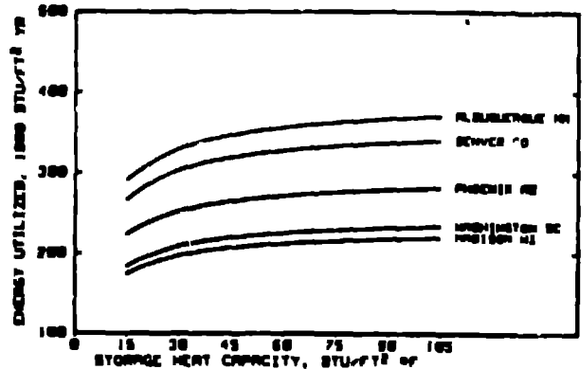

19.b.

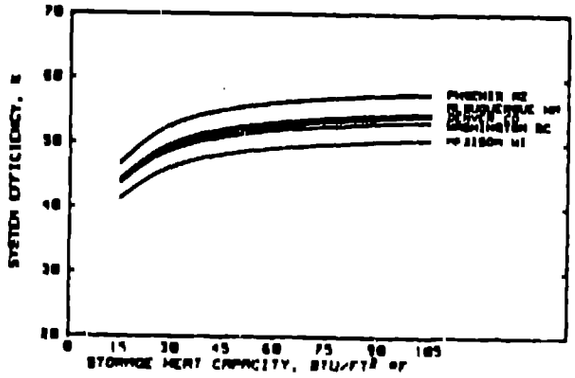

19.c.

Fig. 19a-c. System performance factors for five cities as a function of storage heat capacity.

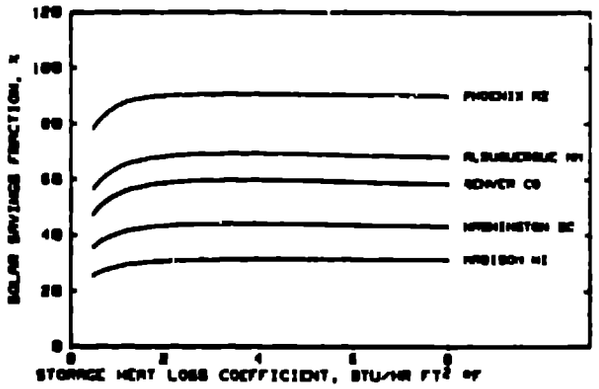

20.a.

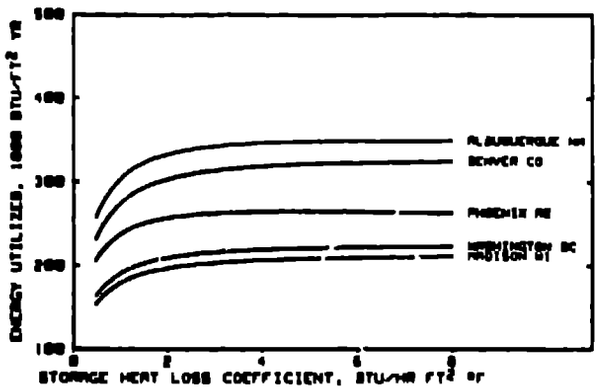

20.b.

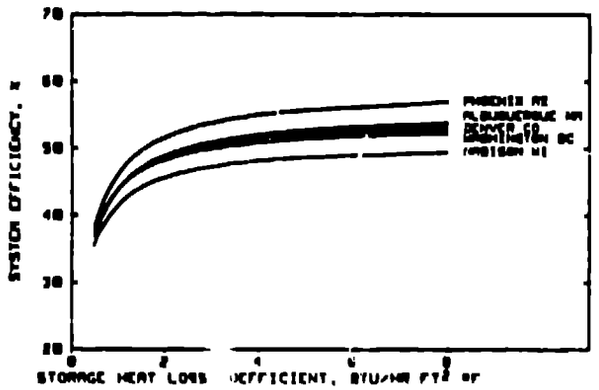

20.c.

Fig. 20a-c. System performance factors for five cities as a function of storage heat-loss coefficient.

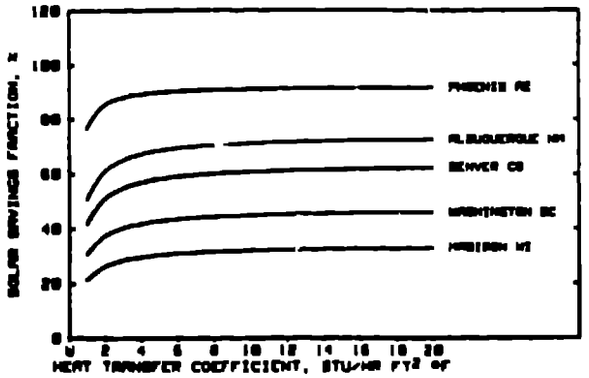

21.a.

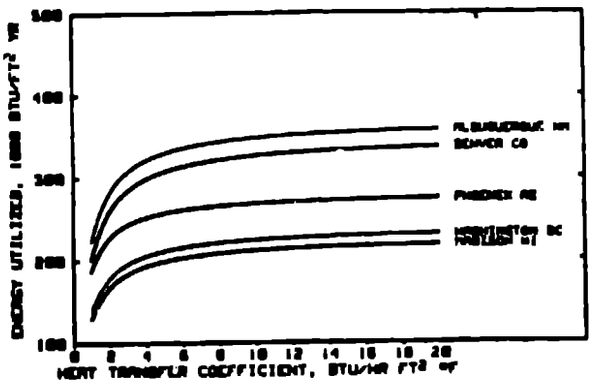

21.b.

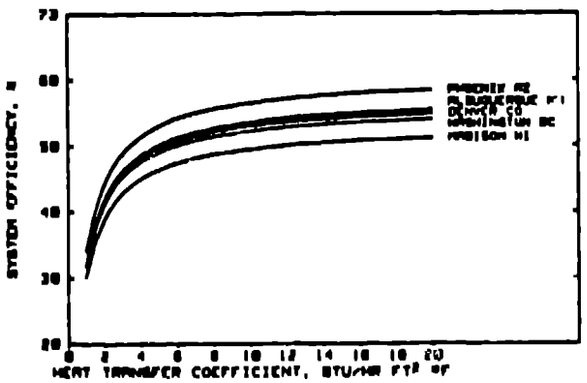

21.c.

Fig. 21a-c. System performance factors for five cities as a function of condenser heat-transfer coefficient.